Electronic version of an article published as International Journal of Bifurcation and Chaos Vol. 17, No. 3, 2007, 837-850,
DOI: 10.1142/S0218127407017586 © World Scientific Publishing Company, https://www.worldscientific.com/worldscinet/ijbc

Bifurcation Analysis of Current Coupled BVP Oscillators

Shigeki Tsuji [*], [†]Tetsushi Ueta [‡], and Hiroshi Kawakami [§]

April 19, 2006

The Bonhöffer-van der Pol (BVP) oscillator is a simple circuit implementation describing neuronal dynamics. Lately the diffusive coupling structure of neurons attracts much attention since the existence of the gap-junctional coupling has been confirmed in the brain. Such coupling is easily realized by linear resistors for the circuit implementation, however, there are not enough investigations about diffusively coupled BVP oscillators, even a couple of BVP oscillators. We have considered several types of coupling structure between two BVP oscillators, and discussed their dynamical behavior in preceding works. In this paper, we treat a simple structure called current coupling and study their dynamical properties by the bifurcation theory. We investigate various bifurcation phenomena by computing some bifurcation diagrams in two cases, symmetrically and asymmetrically coupled systems. In symmetrically coupled systems, although all internal elements of two oscillators are the same, we obtain in-phase, anti-phase solution and some chaotic attractors. Moreover, we show that two quasi-periodic solutions are disappeared simultaneously by the homoclinic bifurcation on the Poincaré map and that a large quasi-periodic solution is generated by the coalescence of these quasi-periodic solutions, but it is disappeared by the heteroclinic bifurcation on the Poincaré map. In the other case, we confirm the existence a conspicuous chaotic attractor in the laboratory experiments.

Keywords: Bifurcation; chaos; BVP oscillator; diffusive coupling

1 Introduction

A circuit equation of Bonhöffer-van der Pol (abbr. BVP) oscillator which is also called FitzHugh-Nagumo model [FitzHugh, 1961; Nagumo 1962] is simplified Hodgkin-Huxley equation [Hodgkin & Huxley, 1952]. Since a BVP oscillator is a simple electric circuit which consists of some simple elements, many researches have investigated not only about the bifurcation phenomena in single BVP oscillator but also about the various coupled BVP systems [Kitajima *et al.*, 1998; Papy & Kawakami, 1995a, 1995b]. When a linear resistor is used for coupling, it means a diffusive coupling. Since a BVP oscillator has two state variables, such as the voltage and current, we have the following several coupling types: voltage-voltage, current-current, voltage-current, and so on. Various synchronous, asynchronous phenomena and some chaotic oscillations may be observed by the interactions of the initial state of each single oscillator and the type of coupling. In these coupled systems, Ueta *et. al* have reported about observed various bifurcation phenomena and some chaotic solutions in the voltage-voltage coupled oscillators [Ueta *et al.*, 2004] and voltage-current coupled oscillators [Ueta *et al.*, 2003]. Additionally, they clarified the regions exhibiting conspicuous phenomena by computing the detailed bifurcation diagrams in the two-parameter space, and showed clearly that these phenomena could be observed in a real circuit.

[*]Dept. Information Science and Intelligent Systems, Tokushima University, Japan
[†]Present affiliation: Aihara Complexity Modelling Project, ERATO, Japan Science and Technology Agency (JST), Japan
[‡]Center for Advanced Information Technology, Tokushima University, Japan
[§]Tokushima University, Japan

In this paper, we study yet another coupling type: current-current coupled BVP oscillator, and focus attention on the complicated behavior produced by relationship between the variation of nonlinearity in individual oscillator and coupling coefficient in this coupling type. Firstly, we analyze the bifurcation structure in a single BVP oscillator by computing the bifurcation diagrams in two parameter space, and apply this information to the analysis of coupled systems. In the following two cases, we investigate bifurcation phenomena and chaotic solutions due to changing parameters of a nonlinear resistor and a linear resistor at the coupling part. We firstly consider a coupled identical oscillators, namely this case is symmetrical coupling. In this case, although all internal elements of two oscillators are the same, we obtain various phenomena depending on the characteristics of nonlinear resistors and coupling coefficient, such as in-phase, anti-phase solution and some chaotic attractors. In addition, we clarify the regions exhibiting these phenomena in the detailed bifurcation diagrams. We show that two quasi-periodic solutions are disappeared simultaneously by the homoclinic bifurcation on the Poincaré map. Furthermore, we find a large quasi-periodic solution with which these quasi-periodic solutions are united, and we also show that this quasi-periodic solution is disappeared by the heteroclinic bifurcation on the Poincaré map. We secondly place different parameter values for each oscillator, i.e., they form an "unbalanced" situation. Since this case is asymmetrical coupling, and this fully four-dimensional system produces some specific bifurcation phenomena. We show bifurcation diagrams of attractors and reveal a conspicuous chaotic attractor like a double scroll [Chua *et al.*, 1986; Chua 1993]. It is confirmed in the laboratory experiments.

2 Bifurcations in Single BVP Oscillator

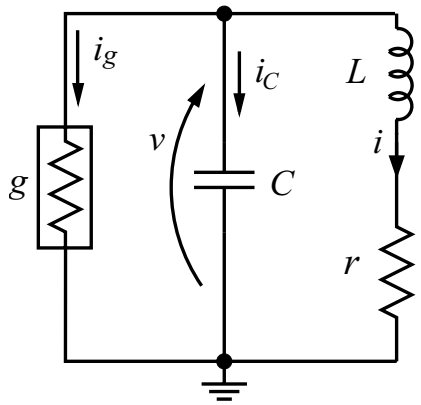

Figure 1: Single BVP oscillator.

To analyze various bifurcation phenomena in a current coupled BVP oscillators, we firstly investigate the bifurcation structures in a single BVP oscillator with nonlinear conductance. Figure 1 shows a simple BVP oscillator without constant voltage source in original BVP oscillator. This circuit equations are described as

$$\begin{cases} \dfrac{dv}{dt} &= \dfrac{1}{C}\left(-i - g(v)\right) \\ \dfrac{di}{dt} &= \dfrac{1}{L}(v - ri). \end{cases} \tag{1}$$

We simply assume the hyperbolic tangent function for $g(v)$ from experimental data of the FET(2SK30A-GR9L) [Ueta *et al.*, 2003; Ueta *et al.*, 2004],

$$g(v) = -\alpha \tanh \beta v. \tag{2}$$

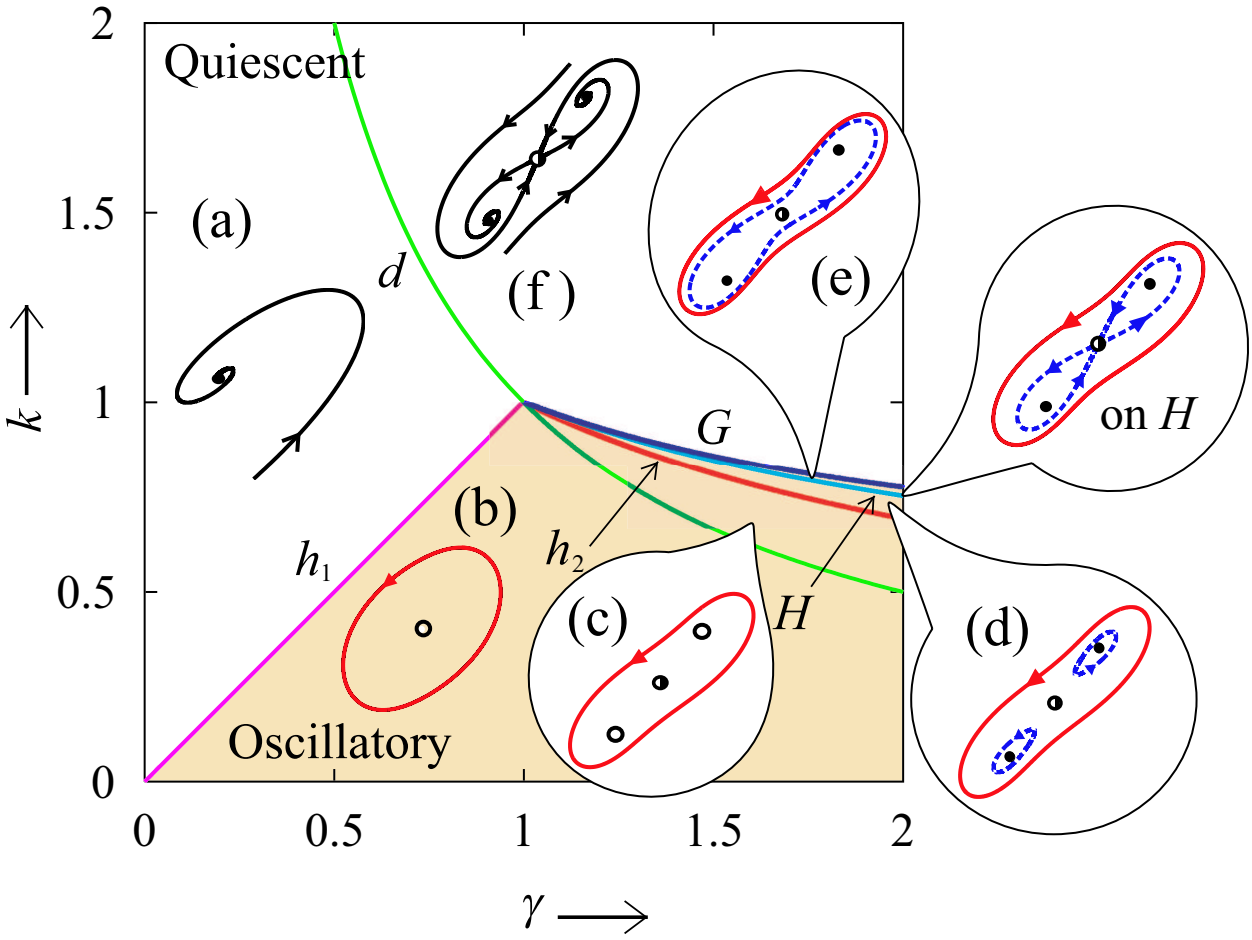

Figure 2: Bifurcation diagram of equilibria and limit cycles in a single oscillator.

Then the following we have normalized equations:

$$\begin{cases} \dfrac{dx}{d\tau} &= -y + \tanh \gamma x \\ \dfrac{dy}{d\tau} &= x - ky, \end{cases} \tag{3}$$

where,

$$\tau = \frac{1}{\sqrt{LC}}t, \quad x = \frac{1}{\alpha}\sqrt{\frac{C}{L}}v, \quad y = \frac{1}{\alpha}i, \quad \gamma = \alpha\beta\sqrt{\frac{L}{C}}, \quad k = r\sqrt{\frac{C}{L}}. \tag{4}$$

From experimental results of a nonlinear conductance using an FET, we can determine parameter values:

$$\alpha = 6.0762 \times 10^{-3}, \quad \beta = 0.3725.$$

We also fix parameters as

$$L = 10.0[\mathrm{mH}], \quad C = 0.022[\mu\mathrm{F}].$$

Figure 2 shows a bifurcation diagram of equilibria and limit cycles observed in the system (3) at the γ-k plane. In this bifurcation diagram, h_1, h_2 and d indicate supercritical Andronov-Hopf, subcritical Andronov-Hopf and pitchfork bifurcations, respectively. G and H indicate tangent bifurcation and homoclinic loop of limit cycle. Here, subscript number of these symbols is a nominal number for classification.

Figure 2 is divided into six regions by the bifurcation curves, and these regions are topologically classified as follows:

Region (a) : only a stable equilibrium (origin) exists.

Region (b) : an unstable equilibrium (origin) and a stable limit cycle coexist.

Region (c) : two unstable equilibria, a saddle (origin) and a stable limit cycle coexist.

Region (d) : two unstable equilibria, a saddle (origin), a stable limit cycle and two unstable limit cycles coexist.

Region (e) : two unstable equilibria, a saddle (origin), a stable limit cycle and an unstable limit cycle coexist.

Region (f) : two unstable equilibria and a saddle (origin) coexist.

To investigate the coupled systems, we utilize these topological information after the following section.

3 Current Coupled BVP Oscillators

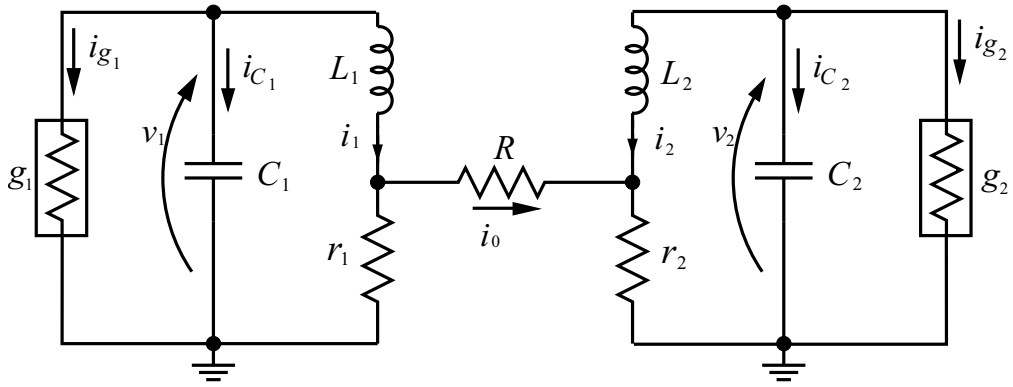

Figure 3: Current coupled BVP oscillators.

We consider the coupled BVP oscillators by a linear resistor with current ports shown as Fig.3. The circuit equations are described as follows:

$$\begin{cases} \dfrac{dv_1}{dt} &= \dfrac{1}{C_1}\left(-i_1 - g_1(v_1)\right) \\ \dfrac{di_1}{dt} &= \dfrac{1}{L_1}\left(v_1 - r_1 i_1 + \dfrac{Gr_1}{1+G(r_1+r_2)}(r_1 i_1 - r_2 i_2)\right) \\ \dfrac{dv_2}{dt} &= \dfrac{1}{C_2}\left(-i_2 - g_2(v_2)\right) \\ \dfrac{di_2}{dt} &= \dfrac{1}{L_2}\left(v_2 - r_2 i_2 + \dfrac{Gr_2}{1+G(r_1+r_2)}(r_2 i_2 - r_1 i_1)\right). \end{cases} \tag{5}$$

where $G = 1/R$, and we fix parameters $L = L_1 = L_2$, $C = C_1 = C_2$, and $r = r_1 = r_2$. One can see that current variables are coupled in these equations. Here, we apply the following transformations:

$$\tau = \frac{1}{\sqrt{LC}}t, \quad x_j = \frac{1}{\alpha}\sqrt{\frac{C}{L}}v_j, \quad y_j = \frac{1}{\alpha}i_j, \tag{6}$$

and

$$\gamma_j = \alpha_j \beta_j \sqrt{\frac{L}{C}}, \quad k = r\sqrt{\frac{C}{L}}, \quad \delta = \frac{Gr}{1+2Gr}, \quad j = 1, 2. \tag{7}$$

Then, we have normalized equations as follows:

$$\begin{cases} \dfrac{dx_1}{d\tau} &= -y_1 + \tanh \gamma_1 x_1 \\ \dfrac{dy_1}{d\tau} &= x_1 - k y_1 + \delta k (y_1 - y_2) \\ \dfrac{dx_2}{d\tau} &= -y_2 + \tanh \gamma_2 x_2 \\ \dfrac{dy_2}{d\tau} &= x_2 - k y_2 + \delta k (y_2 - y_1) \end{cases} \tag{8}$$

We investigate the bifurcation phenomena of two cases whose nonlinear negative conductances of two BVP oscillators are equivalent or else. In the following analysis, we provide that the parameter k of both oscillators are the same value. Additionally, we firstly assume $\gamma = \gamma_1 = \gamma_2$, and compute the bifurcation diagram in the γ-δ plane, i.e., this indicates fully symmetrical coupling. Although symmetrical coupling may seem to be singular case, it is important to investigate dynamical behavior of this case since the dynamical behavior and topological properties of asymmetrically coupled systems is evolved and conjectured from results of analysis for symmetrically coupled systems. As the second case, we fix the parameter γ_1, and compute the bifurcation diagram in the γ_2-δ plane, i.e., this case indicates asymmetrical coupling except for $\gamma_1 = \gamma_2$ line in the bifurcation diagram.

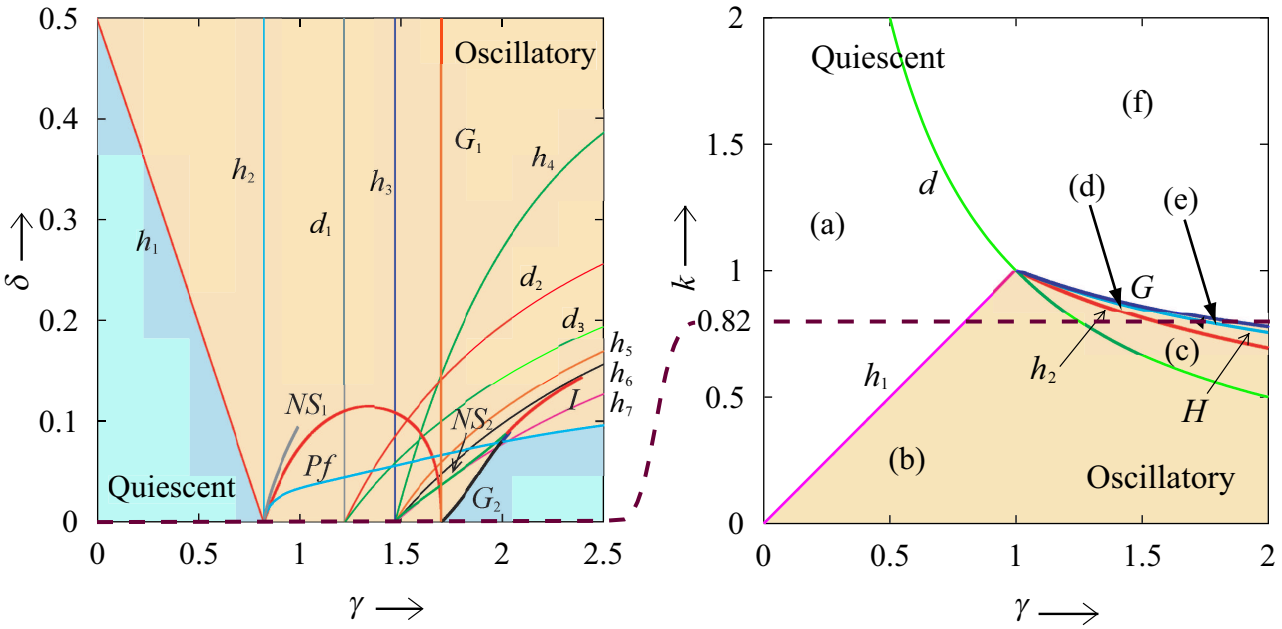

(A): Coupled BVP oscillators (B): Single BVP oscillator

Figure 4: Bifurcation diagram of equilibria and limit cycles.

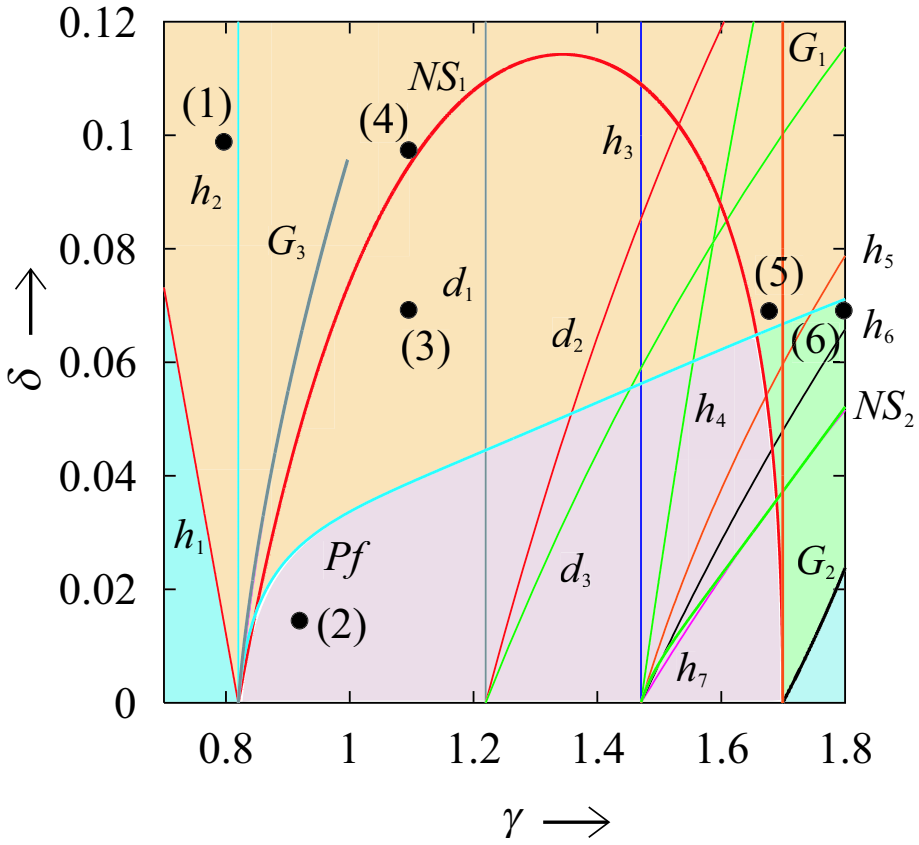

Figure 5: Enlarged bifurcation diagram of Fig. 4-(A).

4 Bifurcations in γ-δ plane

We set the nonlinear conductance parameters $\gamma = \gamma_1 = \gamma_2$, and solve the bifurcation diagram in γ-δ plane as shown in Fig.4-(A). h and d indicate Andronov-Hopf, and pitchfork bifurcations of equilibrium respectively. Additionally, G, I, NS and Pf indicate tangent, period-doubling, Neimark-Sacker and pitchfork bifurcations of periodic solutions, respectively. Various bifurcation curves exist in this diagram intricately. However, these curves are converged on some points of $\delta = 0$ line. Notice that $\delta \to 0$ means decoupling of oscillators. In this case, the parameter k of each oscillator is fixed to 0.82, i.e., $\delta = 0$ line is corresponding to $k = 0.82$ line in Fig.4-(B). Therefore, to changing the parameter γ from $\gamma = 0$, topological structure of each single oscillator changes from (a) to (f) via some bifurcations in Fig.4-(B). Each intersecting point corresponds to four convergence points in Fig.4, i.e., four bifurcation curves cross $k = 0.82$ line in Fig.2. However, although we do not solve the homoclinic bifurcations derived from convergence point, five convergence points exist in a normal situation. For these reasons, some bifurcations are generated from five convergence points due to increasing the parameter δ.

The state of each oscillator is quiescent in the left side of Fig.4-(A). There is only generated the oscillation state of anti-phase synchronization via Andronov-Hopf bifurcation h_1 as shown in Fig.6-(1). Moreover, since other bifurcations which generate the stable limit cycles do not exist, only anti-phase solution exists in the upper side of Fig.4-(A). When coupling intensity is strong comparatively, thus, a stable anti-phase solution is widely observed in this coupled oscillators, and it differs in contrast with the voltage coupled oscillators [Ueta *et al.*, 2004]. There exist various bifurcations of limit cycles in the under side of Fig.4-(A). Figure 5 shows enlargement in the under side of Fig.4-(A). The anti-phase solution

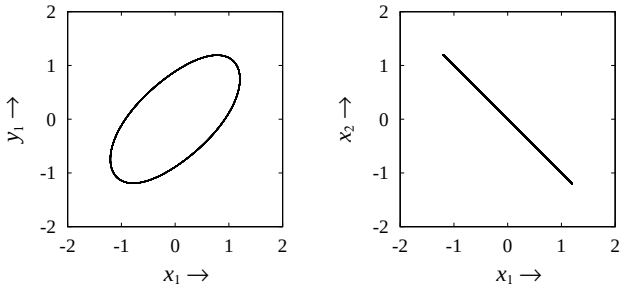

(1) : $\gamma = 0.8,\ \ \delta = 0.1$

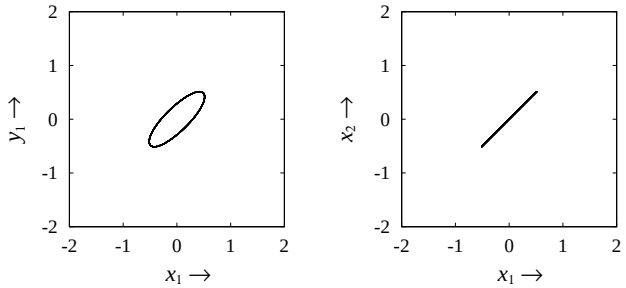

(2) : $\gamma = 0.86,\ \ \delta = 0.015$

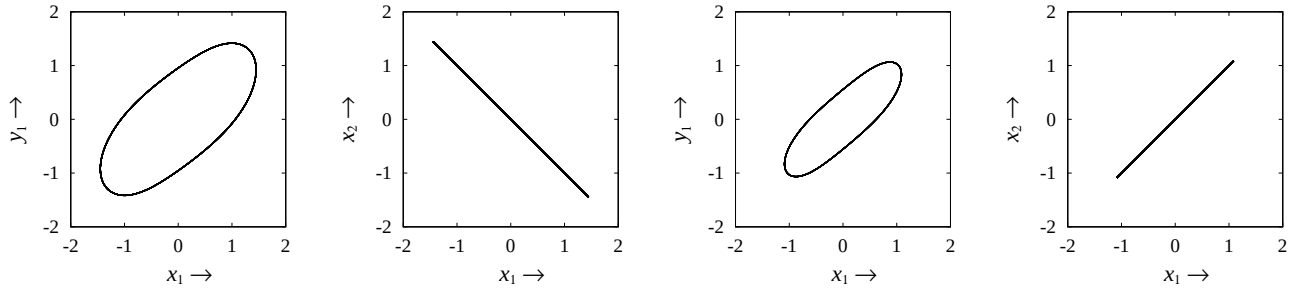

(3) : $\gamma = 1.1,\ \ \delta = 0.07$

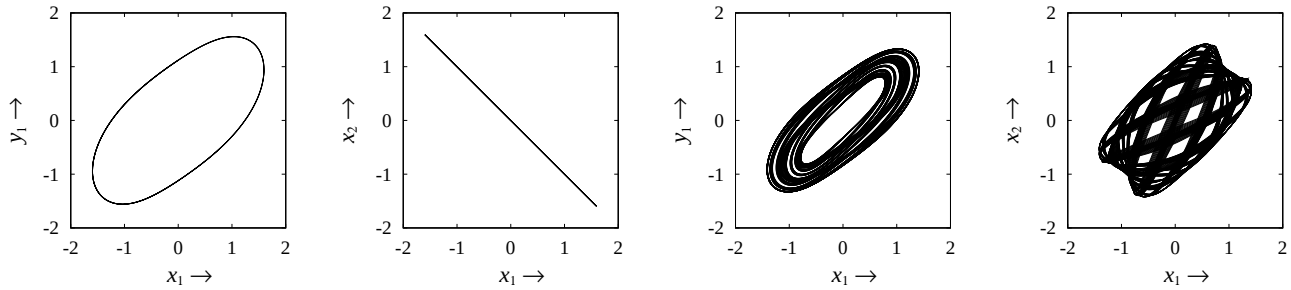

(4) : $\gamma = 1.1,\ \ \delta = 0.0954$

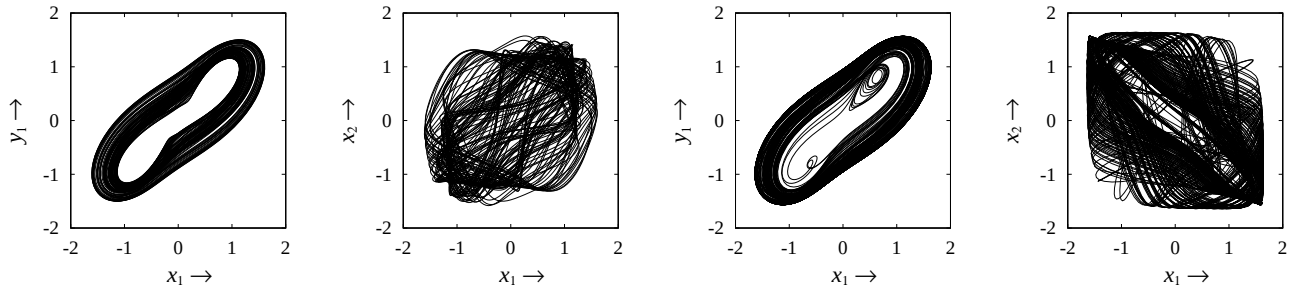

(5) : $\gamma = 1.665,\ \ \delta = 0.068$

(6) : $\gamma = 1.8,\ \ \delta = 0.068$

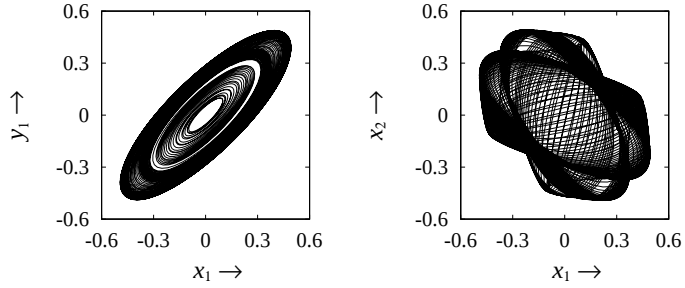

(7) : $\gamma = 0.835,\ \ \delta = 0.01$

Figure 6: Phase portraits of coupled oscillators in Fig.5.

observed on the point (1) as shown in Fig.6-(1), but it becomes unstable via Pf. On the other hand, unstable limit cycle generated by h_2, and it changes to a stable limit cycle (in-phase solution) via NS_1. This solution (Fig.6-(2)) is only observed in the shaded region including the point (2). However, in the region including the point (3), anti-phase and in-phase solutions coexist as shown in Fig.6-(3). In the point (4), anti-phase and quasi-periodic solutions coexist. This quasi-periodic solution is not generated by NS_1, and it changes to chaotic solution via tours breakdown although all parameters of two oscillators are the same, but it is disappeared instantly then the state of this system changes to a stable anti-phase solution. In other points, a chaotic solution is observed as shown in Fig.6-(5) and Fig.7-(1), and a stable anti-phase solution also exists in the point (5). By changing the parameter γ, a chaotic solution is disappeared by boundary crisis. The state of this system switches to a stable anti-phase solution. In the point (6), however, a stable anti-phase solution becomes unstable via Pf then the state of this system changes into other chaotic solution as shown in Fig.6-(6) and Fig.7-(2). Figure 8 shows the Lyapunov exponents including the point Fig.6-(5) and (6). In these points, it is true that largest Lyapunov exponent is positive value.

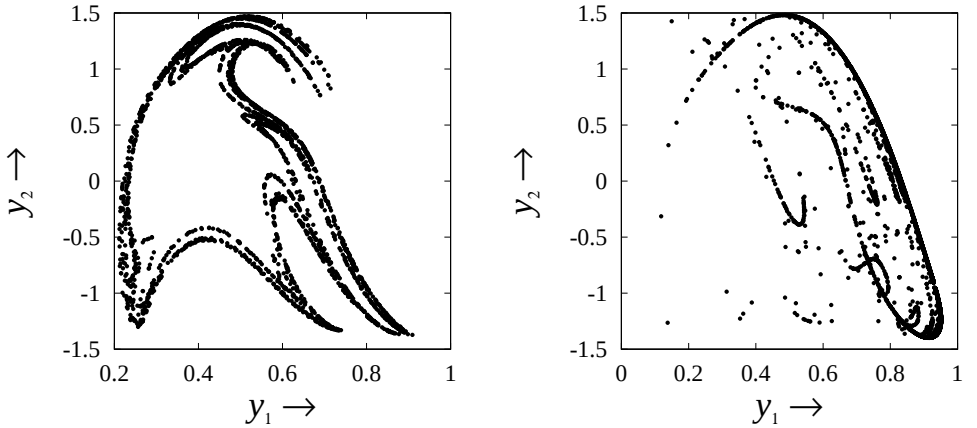

Figure 7: The Poincaré maps ($x_1 = 0$) corresponding to Fig. 6-(5) and (6).

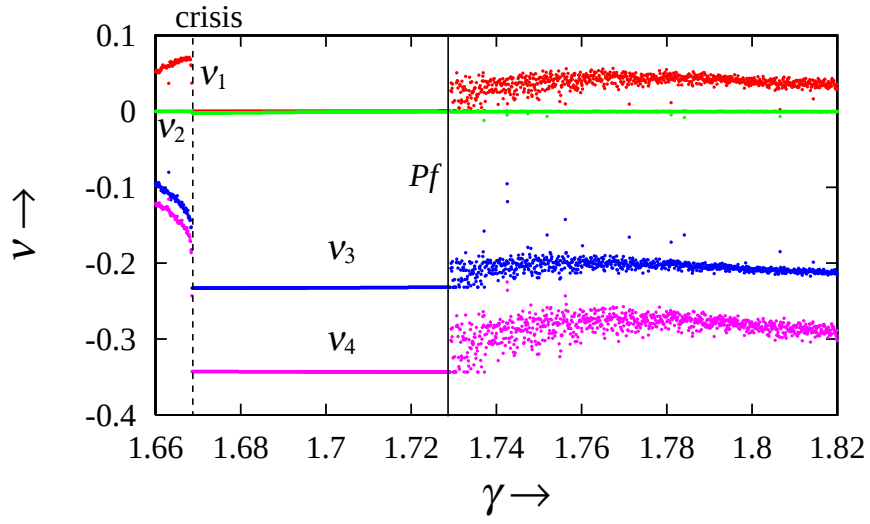

Figure 8: Lyapunov exponents, $\delta = 0.068$.

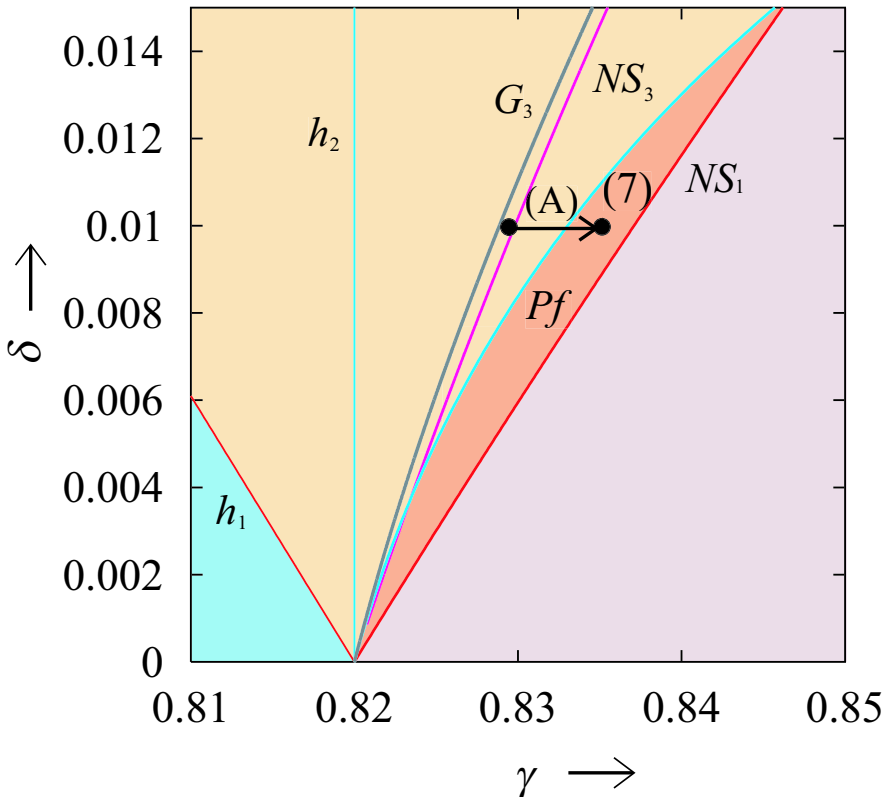

Figure 9: Enlarged bifurcation diagram of Fig. 5.

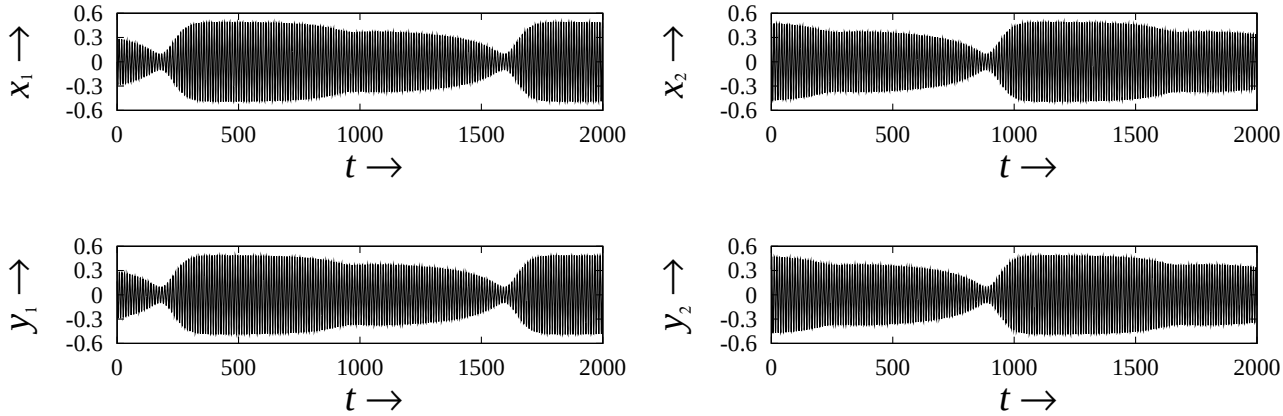

Figure 10: Wave forms in the point (7) of Fig. 9.

Figure 9 shows the enlargement of Fig.5 where δ is comparatively small. A solution changing between two states is observed on the point (7) as shown in Fig.6-(7) and Fig.10. To investigate the generating processes of this mode, we observe the topological structure in some points of neighborhood region as shown in Fig.11, and show that schematic diagram of topological structure on the line (A) in Fig.12. In addition, Fig.13 shows the Lyapunov exponents on the line (A).

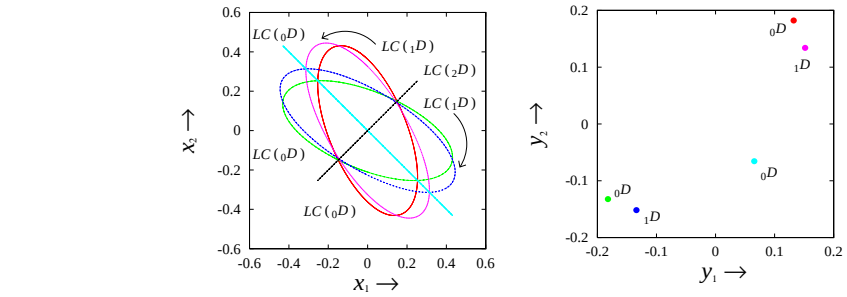

(1) : $\gamma = 0.8291,\ \ \delta = 0.01$

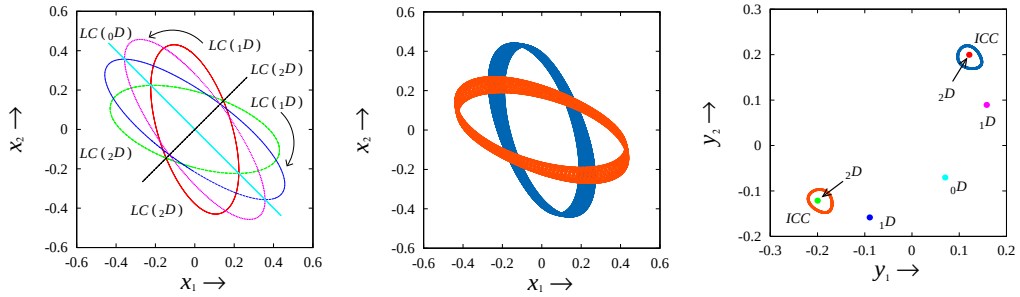

(2) : $\gamma = 0.83,\ \ \delta = 0.01$

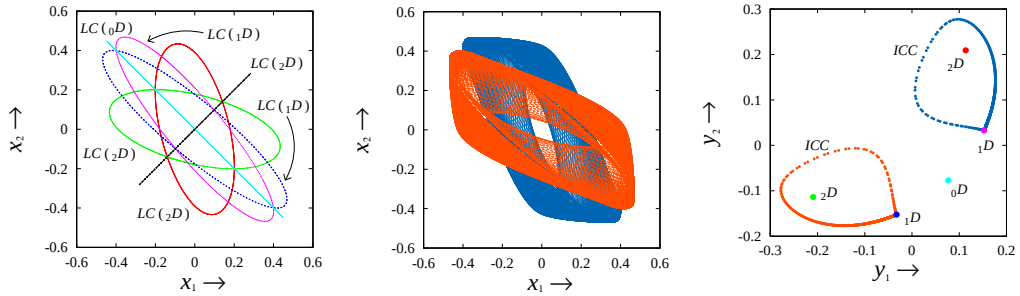

(3) : $\gamma = 0.83135,\ \ \delta = 0.01$

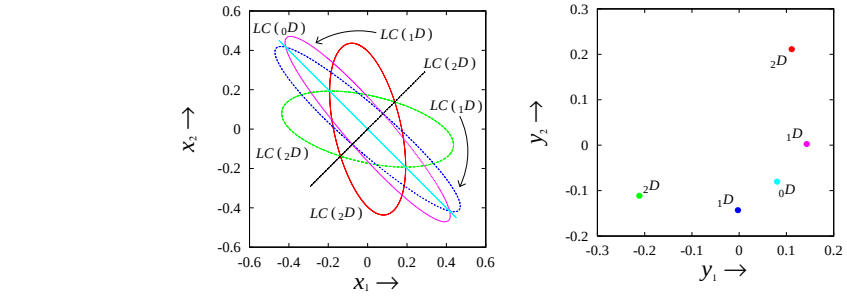

(4) : $\gamma = 0.832,\ \ \delta = 0.01$

Figure 11: Phase portraits (x_1-x_2) and the Poincaré map (y_1-y_2) of some points on the line (A) in Fig.9. The Poincaré section is $x_1 - x_2 + 0.4 = 0$. ${}_kD(k = 0, 1, \cdots, 4)$ denotes a "direct" type of hyperbolic fixed point, and the superscript and subscript numbers indicate the period of limit cycle and the dimension of the unstable subspace respectively. ICC and $LC({}_kD)$, moreover, denote the invariant closed curve and the orbit of limit cycle corresponding to each fixed point respectively [Kawakami, 1984].

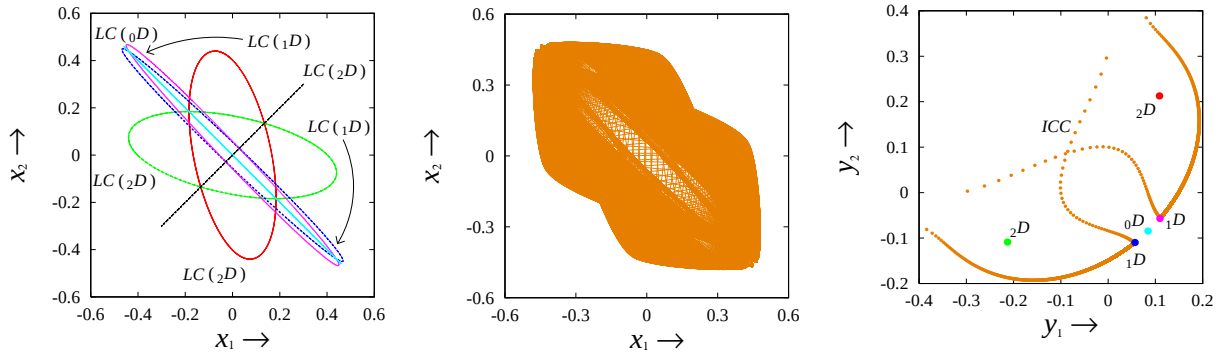

(5) : $\gamma = 0.8329,\ \ \delta = 0.01$

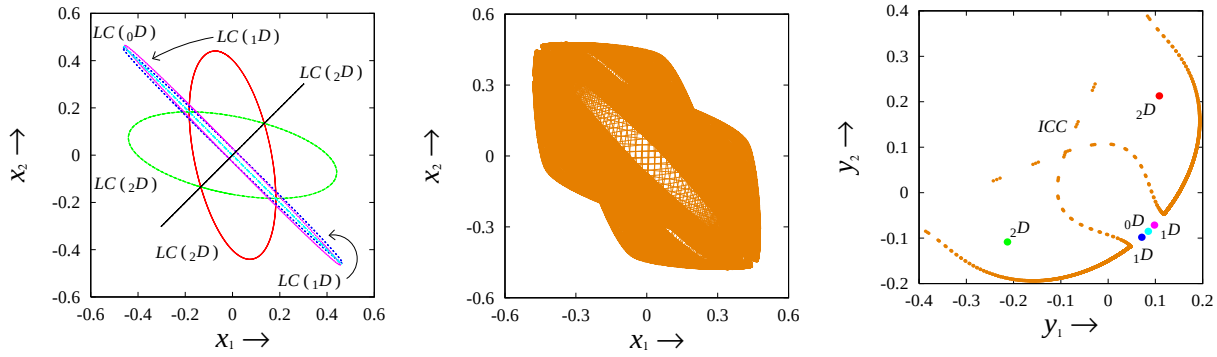

(6) : $\gamma = 0.833,\ \ \delta = 0.01$

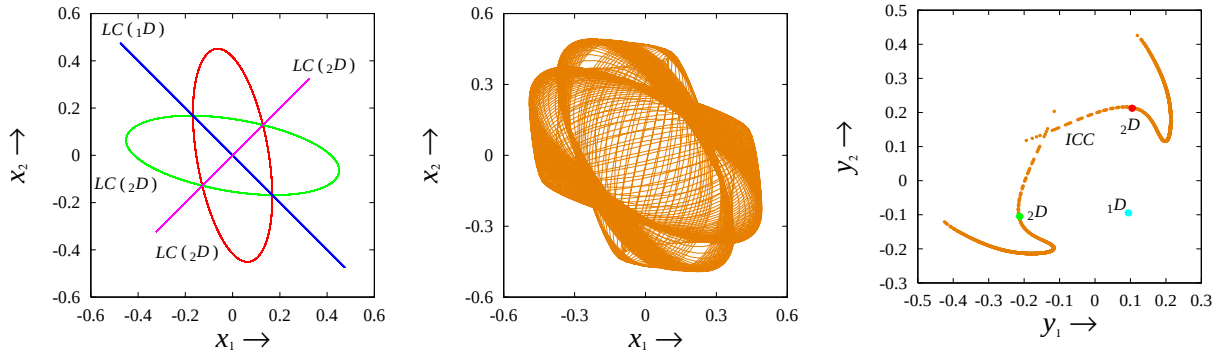

(7) : $\gamma = 0.835,\ \ \delta = 0.01$

Figure 11: (*Continued*)

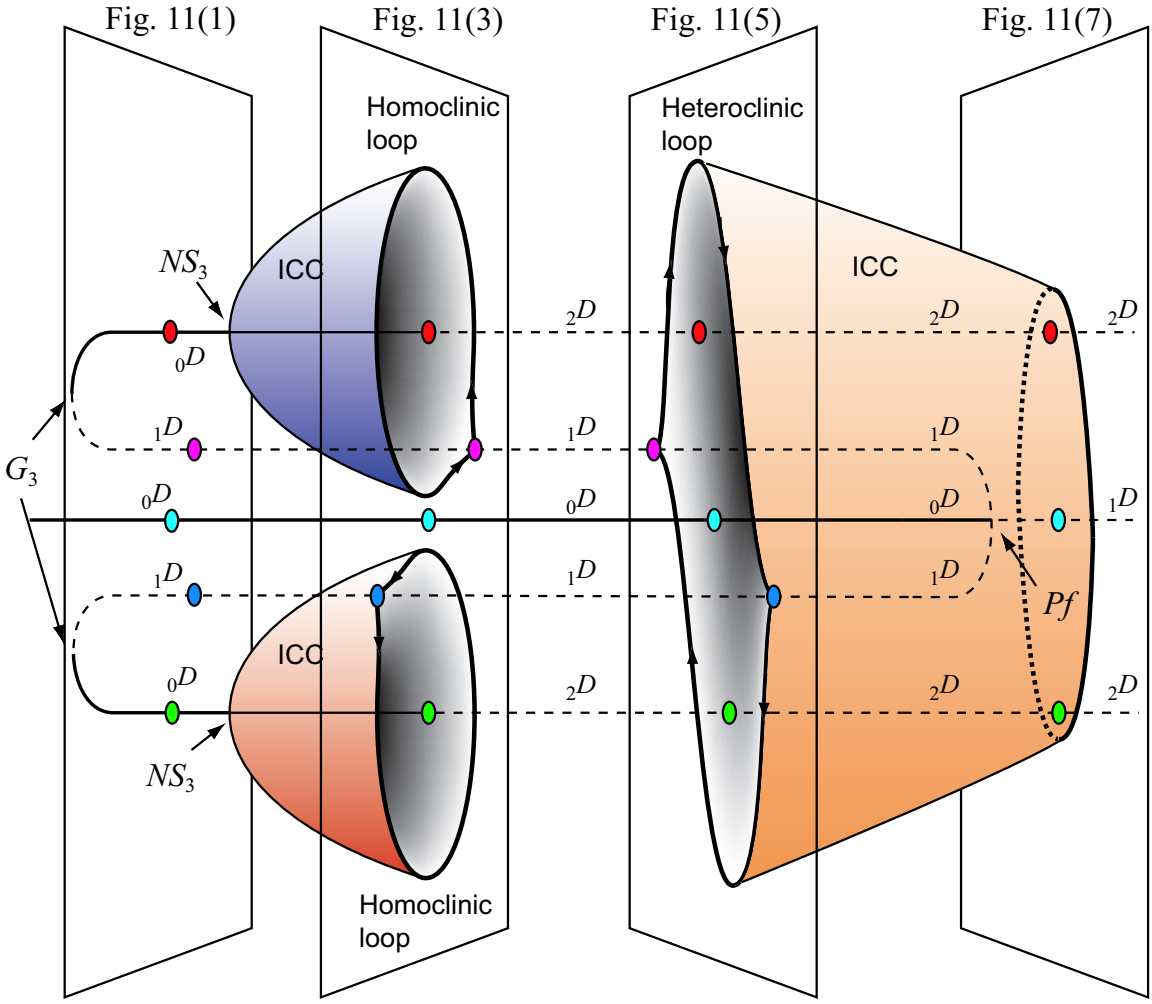

Figure 12: Schematic diagram of topological structure on the line (A) in Fig.9.

On the start point of the arrow line (A) in Fig.9, a phase portrait is shown Fig.11-(1). In this region, a stable anti-phase and an unstable in-phase solutions coexist. Moreover, two stable limit cycles and two unstable limit cycles exist except for above solutions. As the parameter γ changes along the direction of the arrow, two quasi-periodic solutions are generated simultaneously from two stable limit cycles ($2 \times LC(_0D)$) via NS_3, as shown in Fig.11-(2). These quasi-periodic solutions show the invariant closed curves (ICCs) on the Poincaré map. By increasing the parameter γ from 0.83, two ICCs become large gradually on the Poincaré map, and these ICCs contact with each $_1D$ point of unstable limit cycles as shown in Fig.11-(3), i.e., on the Poincaré map, homoclinic bifurcation is generated. For this reason, two quasi-periodic solutions are disappeared immediately as shown in Fig.11-(4).

A large-amplitude quasi-periodic solution is generated as shown in Fig.11-(5), (6) and (7). This solution seems the behavior which two quasi-periodic solutions united. On the Poincaré map, heteroclinic bifurcation is generated as shown in Fig.11-(5), and the ICC is disappeared by this bifurcation as shown in Fig.11-(4) and 12. On the other hand, a stable anti-phase solution changes to an unstable solution, and two unstable limit cycles ($2 \times LC(_1D)$) are disappeared by Pf. Here, all remaining solutions are unstable solutions except for a large-amplitude quasi-periodic solution as shown in Fig.11-(7). In the point (7), although ICC seems to be in contact with two $_2D$ points of unstable limit cycles, as shown in Fig.12, it is not in contact with them. As this large-amplitude quasi-periodic solution changes to the

form of simple torus gradually, it shows the behavior which approximated to in-phase solution rather than anti-phase solution as it approaches NS_1, as shown in Fig.11-(7), but this solution is not generated by NS_1. In fact, quasi-periodic solution generated by NS_1 does not exist stably in this case. Additionally, in the right-side of NS_1, a large-amplitude quasi-periodic and in-phase solutions coexist, but the state of this system changes to a stable in-phase solution eventually as shown in Fig.13.

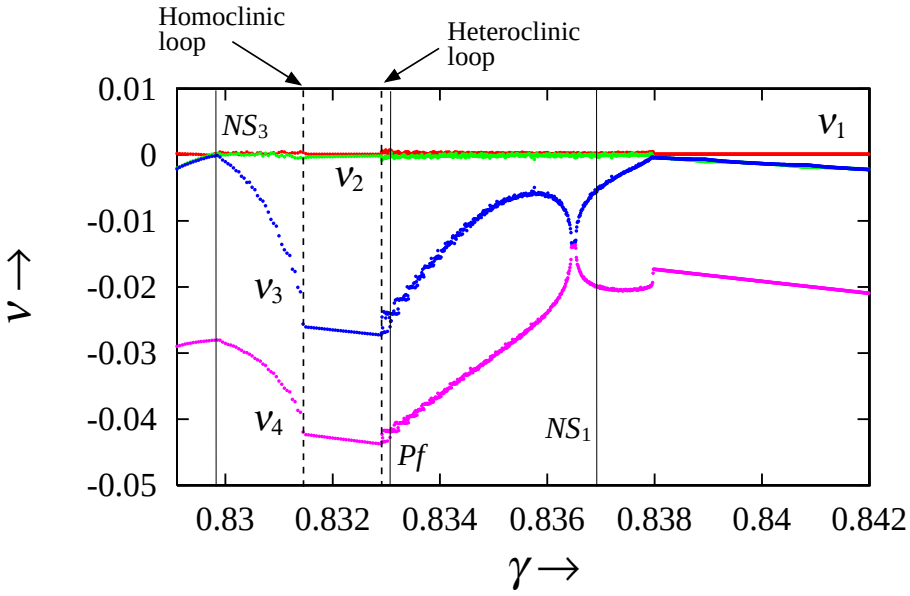

Figure 13: Lyapunov exponents along the arrow line (A) in Fig.9.

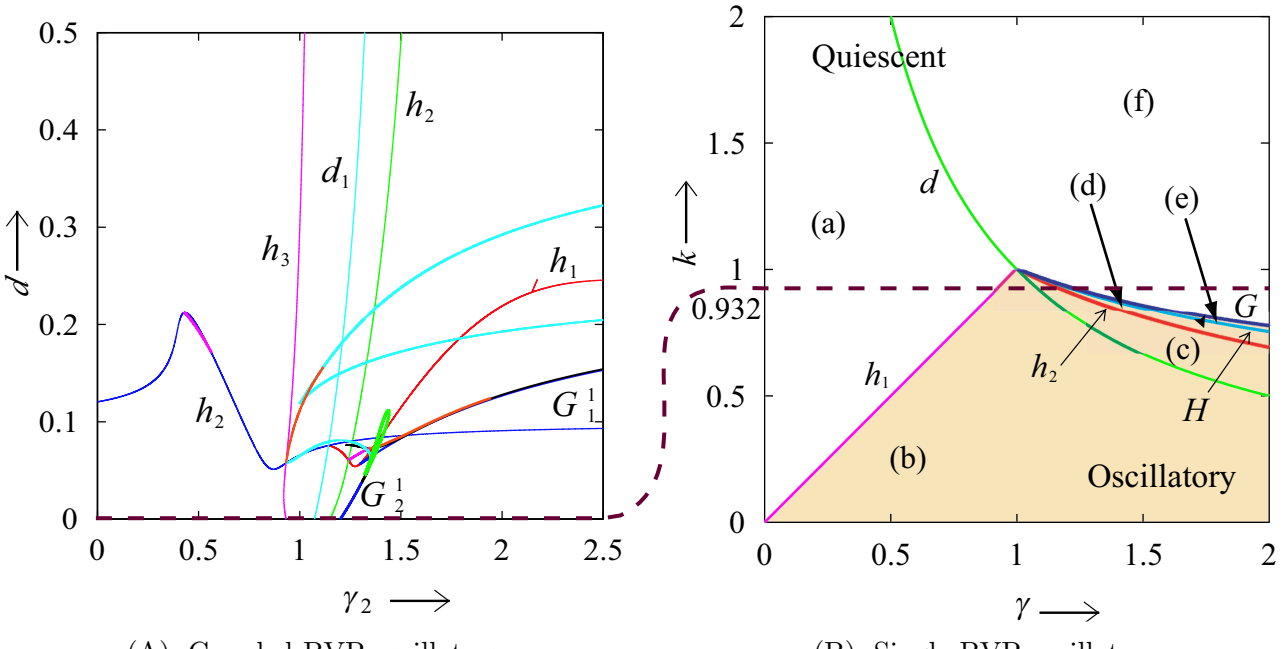

(A): Coupled BVP oscillators

(B): Single BVP oscillator

Figure 14: Bifurcation diagram of equilibria and limit cycles.

5 Bifurcations in γ_2-δ Plane

Finally, we fix the k as 0.932, and set the parameter of odd oscillator as $(\gamma_1, k) = (0.825, 0.932)$. In this case, this oscillator shows only one stable equilibrium in the region (a) of Fig.2, and other oscillator shows all phenomena in Fig.2 by changing the value of γ_2. That is to say, this case is asymmetrical coupling except for $\gamma_1 \neq \gamma_2$. For this reason, more complicated bifurcation structure would be shown compared with the previous case. We obtain the bifurcation diagram in γ_2-δ plane as shown in Fig.14. The line of $\delta = 0$ in Fig.14-(A) corresponds to $k = 0.932$ line in Fig.14-(B). Moreover, $\gamma_2 = 0.825$ line in Fig. 14-(A) corresponds to $\gamma = 0.825$ line in Fig. 4-(A). Additionally, some convergence points of the bifurcation curves and $\delta = 0$ line exist such the previous case, but some bifurcation curves do not in contact with the $\delta = 0$ line by reason of that this case is asymmetrical coupling. Here, we attend to the bifurcation phenomena by these curves in Fig.15. Two small stable period-1 solutions (Fig.16-(1)) exist in the start point of the arrow line (A) of Fig.15, and a stable equilibrium exists in the neighborhood of each limit cycle. Moreover, when we set the parameter δ as 0, the state of each oscillator on this line corresponds to the state in the region (a) $(\gamma_1, k) = (0.825, 0.932)$ and (f) $(\gamma_2, k) = (1.37, 0.932)$ in Fig.2, respectively. That is, although the states of both of oscillators are different, they do not oscillate. When increasing the parameter δ in the direction of the arrow, these period-1 solutions change to period-2 (Fig.16-(2)) via period-doubling bifurcation I_1^1. These period-2 solutions change to quasi-periodic (Fig.16-(3)) via NS_1^2, and thereafter they become single chaotic solutions (Fig.16-(4)) via torus breakdown. However, since two chaotic solutions is disappeared by boundary crisis, the state of this system changes to two stable equilibria. These stable equilibria switch to unstable via h_1, then the state of this system shows a large chaotic solution (Fig.16-(5)) changing between single chaotic solutions like a double scroll attractor [Chua *et al.*, 1986; Chua, 1993]. Figure 17 shows a snap shot of an oscilloscope measuring $r_1 i_1$-$r_2 i_2$ in Eq.(5). All stable attractors found in the system (Eq.(8)) are confirmed by a real circuit.

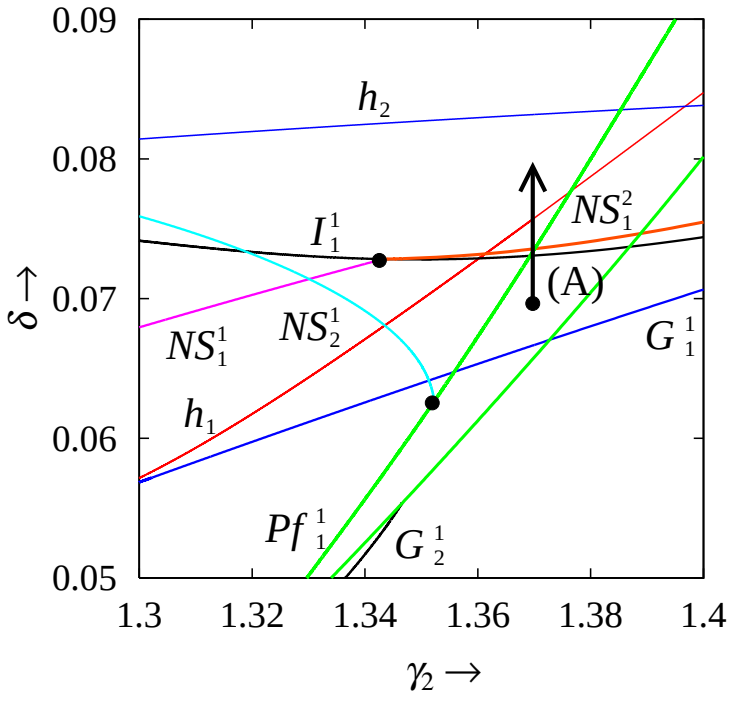

Figure 15: Enlarged bifurcation diagram of Fig. 14-(A).

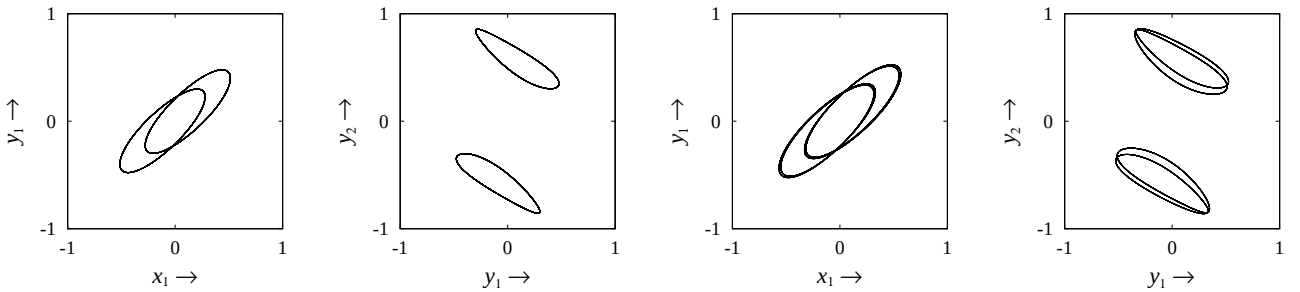

(1) : $\gamma_2 = 1.37,\ \delta = 0.07$ (2) : $\gamma_2 = 1.37,\ \delta = 0.0733$

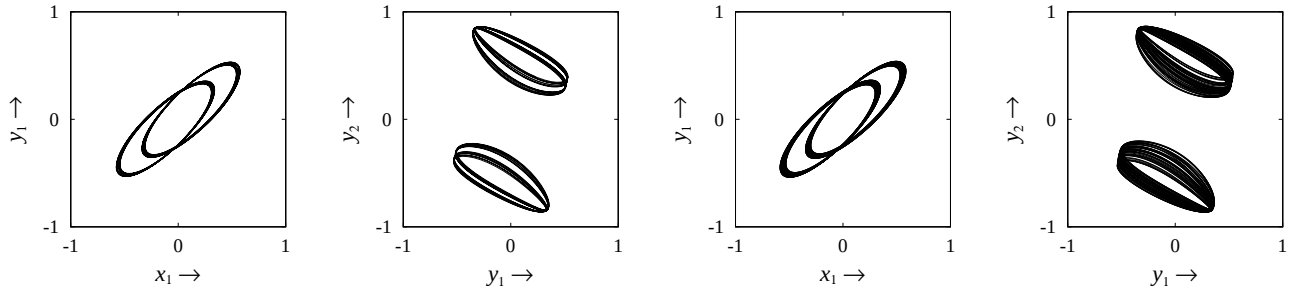

(3) : $\gamma_2 = 1.37,\ \delta = 0.0736$ (4) : $\gamma_2 = 1.37,\ \delta = 0.0739$

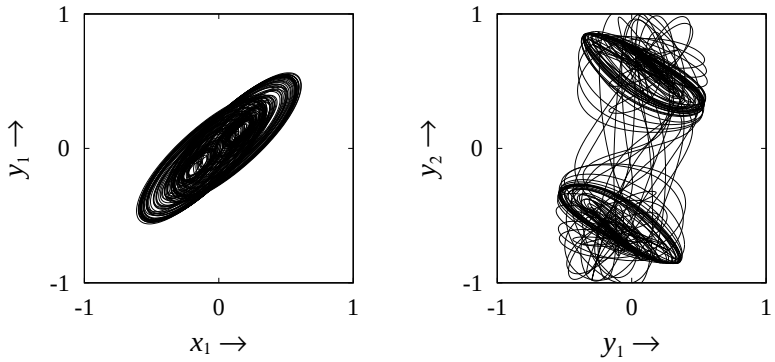

(5) : $\gamma_2 = 1.37,\ \delta = 0.076$

Figure 16: Phase portraits of coupled oscillators in Fig. 15.

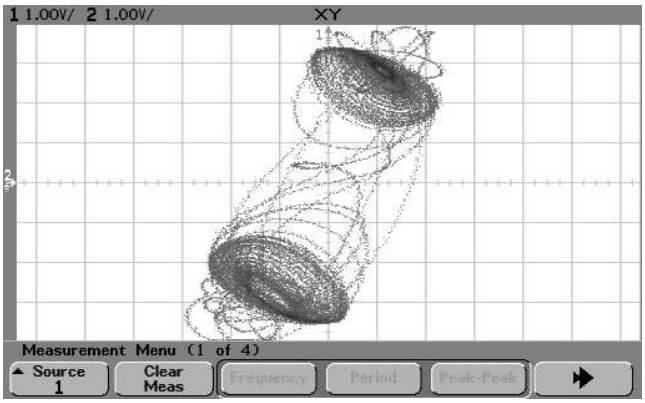

Figure 17: Laboratory experiment according to the simulation result of Fig. 16-(5). $L = 10.0$[mH], $C = 0.022[\mu\text{F}]$, $r \approx 630[\Omega]$, $R \approx 7000[\Omega]$, 1[V/div].

6 Conclusions

In this paper, we analyzed a current coupled BVP oscillators about two cases. Firstly, we showed that various bifurcation phenomena and some chaotic solutions are observed by changing the values of nonlinear resistor and linear resistor using for coupling, although the values of each internal element of two oscillator are the same. We computed the bifurcation diagrams and clarified the two-parameter space exhibiting each solution, in-phase, anti-phase, quasi-periodic and chaotic solutions. Moreover, we showed that homoclinic and heteroclinic loops are generated on the Poincaré map. By these global bifurcations, quasi-periodic solutions is disappeared. As the second case, when each oscillator has different internal nonlinear resistor, we found that the behavior switching two single chaotic solutions alternatively shown also by Ref. [Ueta *et al.*, 2004], and we confirmed that this solution is shown in a real circuit.

References

[1] Chua, L. O., Komuro, M. & Matsumoto, T. [1986] "The double scroll family," *IEEE Trans. Circuits Syst.* **CAS-33**, 1073–1118.

[2] Chua, L. O. [1993] "Global unfolding of Chua's circuit," *IEEE Trans.* **76-A**, 704–734.

[3] FitzHugh, R. [1961] "Impulses and physiological state in theoretical models of nerve membrane," *Biophy. J.* **1**, 445–467.

[4] Hodgkin, A. L. & Huxley, A. F. [1952] "A qualitative description of membrane current and its application to conduction and excitation in nerve," *J. Physiol.* **117**, 500–544.

[5] Kawakami, H. [1984] "Bifurcation of periodic responses in forced dynamic nonlinear circuits: computation of bifurcation values of the system parameters," *IEEE Trans. Circuits and Systems*, **CAS-31**, 246–260.

[6] Kitajima, H., Katsuta, Y. & Kawakami, H. [1998] "Bifurcations of periodic solutions in a coupled oscillator with voltage ports," *IEICE Trans. Fundamentals*, **E81-A**, 476–482.

[7] Nagumo, J., Arimoto, S. & Yoshizawa, S. [1962] "An active pulse transmission line simulating nerve axon," In *Pro. of IRE* **50**, 2061–2070.

[8] Papy, O. & Kawakami, H. [1995a] "Symmetrical properties and bifurcations of the periodic solutions for a hybridly coupled oscillator," *IEICE Trans. Fundamentals*, **E78-A**, 1816–1821.

[9] Papy, O. & Kawakami, H. [1995b] "Symmetry breaking and recovering in a system of n hybridly coupled oscillators," *IEICE Trans. Fundamentals*, **E79-A**, 1581–1586.

[10] Ueta, T. & Kawakami, H. [2003] "Bifurcation in asymmetrically coupled BVP oscillators," *International Journal of Bifurcation and Chaos* **13**, 1319–1327.

[11] Ueta, T., Miyazaki, H., Kousaka, T. & Kawakami, H. [2004] "Bifurcation and chaos in coupled BVP oscillators," *International Journal of Bifurcation and Chaos* **14**, 1305–1324.